In-situ gravimetry of nickel thin film during potentiodynamic polarization in acidic and alkaline sulfate solutions

Naoki Kikuchi and Masahiro Seo*

Graduate School of Engineering, Hokkaido University

Kita-13 Jo, Nishi-8 Chome, Kita-ku, Sapporo 060-8628, Japan

*Corresponding author : Masahiro Seo

Graduate School of Engineering, Hokkaido University

Kita-13 Jo, Nishi-8 Chome, Kita-ku, Sapporo 060-8628, Japan

Tel. /Fax : +81-11-706-6735

E-mail : seo@elechem1-mc.eng.hokudai.ac.jp

Abstract

The passivation process of nickel thin films during potentiodynamic polarization in acidic and alkaline sulfate solutions was analyzed by an electrochemical quartz crystal microbalance (EQCM) to separate the partial current density of nickel dissolution through the passive film, $i_{Ni^{2+}}$, and the partial current density of film growth, $i_{O^{2-}}$. The values of $i_{Ni^{2+}}$ and $i_{O^{2-}}$ during potentiodynamic polarization (20 mV s^{-1}) in the passive potential region could be separated by comparing the mass change rate and net polarization current as a function of electrode potential. It is found that $i_{Ni^{2+}}$ is larger than $i_{O^{2-}}$ in pH 3.0, 0.5 M sulfate solution, while the situation reverses in pH 12, 0.5 M sulfate solution. The sulfate concentration dependences of $i_{Ni^{2+}}$ and $i_{O^{2-}}$ in pH 3.0 , sulfate solution were significant as compared to those in pH 12, sulfate solution.

Keywords : A. Nickel Thin Film ; A. Sulfate Solution ; B. EQCM ; C. Passivation ; C. Partial Current ; C. Film Growth.

1. Introduction

An electrochemical quartz crystal microbalance (EQCM) is powerful and useful technique for analysis of passivation process of metal thin film in aqueous solution because it is capable of measuring simultaneously the changes in mass and current. In our previous EQCM study [1,2] of galvanostatic polarization of iron thin film near the corrosion potential in deaerated weakly acidic solution, the anodic current of iron dissolution as ferrous ions could be separated from the cathodic current of hydrogen evolution by comparing the mass change rate and net polarization current.

Vetter and Gorn [3] investigated the passivation process of iron by using a solution analysis combined with coulometry and proved for the first time that the anodic current flowed during anodic passivation is composed of two partial currents of passive film growth and of metal dissolution through the film. We applied EQCM to passivation process of copper thin film and succeeded in separating two partial currents of passive film growth and of copper dissolution through the film [4,5]. Grzegorzewski and Heusler [6] combined a ring-disc electrode with EQM to measure separately the transport rates of Mn^{2+}, O^{2-}, H^{+} and H_2O in MnO_2 film and showed that the exchange current of Mn^{2+} is much larger than that of O^{2-}. Recently, Schmutz *et al.* [7], Olsson *et al.* [8] and Hamm *et al.* [9] have indicated that the thickenss and compositional changes of passive film during anodic polarization of iron-chromium alloys or 304 stainless steels prepared with a physical vapor deposition can be monitored by using EQCM and XPS.

In this study, EQCM was applied to passivation process of nickel thin film during potentiodynamic polarization in acidic and alkaline sulfate solutions to separate two partial currents of passive film growth and nickel dissolution through the film and to discuss the pH and sulfate concentration dependences of these partial currents.

2. Experimental

The nickel films with a thickness of 800 nm were electroplated on one side of gold electrodes of quartz oscillator (5 MHz, AT-cut). The phase-lock oscillator (Maxtek, Inc, PLO-10) was used to monitor the changes in resonant frequency. The mass sensitivity of 5 MHz, AT-cut quartz oscillator is $\Delta m / \Delta f = - 1.77 \times 10^{-8}$ g cm^{-2} Hz^{-1} according to Sauerbrey's equation [6]. The electroplating of nickel was performed under a constant cathodic current density of 10 mA cm^{-2} at 298 K in pH 6, mixed solution of $NiSO_4$, NH_4Cl and H_3BO_3. The electrolytes employed for experiments were pH 3.0 and 12 sulfate solutions with two different concentrations (0.5 M and 0.1 M), which were prepared by mixing Na_2SO_4 and H_2SO_4 or NaOH. The electrolyte solutions of about 100 cm^3 were introduced into an EQCM cell at 298 K and deaerated with ultra-pure argon gas before and during experiments.

The air-formed film on nickel was cathodically reduced at a constant cathodic current density of 10 μA cm^{-2} for 10 min in the electrolyte solution and then the potentiodynamic polarization in the renewed solution was performed at a potential sweep rate of 20 mV s^{-1}. The changes in mass and current during potentiodynamic polarization were measured simultaneously and recorded on a personal computer. The electrode potential of nickel was measured by an Ag/ AgCl reference electrode and converted to a standard hydrogen electrode scale (SHE).

3. Results and Discussion

Figures 1,2,3, and 4 show the voltammograms and gravimetrical curves of nickel thin film in 0.5 M and 0.1 M Na_2SO_4 solutions of pH 3.0 and 12, respectively. The rapid decreases in mass are observed in the active potential region of nickel during anodic potential sweep. The mass decreases still in the passive potential region although the mass loss rates are significantly small as compared to those in the active potential region. In the anodic

potential sweep, the total decreases in mass are larger in pH 3.0 than pH 12 Na_2SO_4 solution, and also larger in 0.5 M than 0.1 M Na_2SO_4 solution. In the cathodic potential sweep from the anodic potential limit, the slight decreases in mass are observed in pH 3.0, Na_2SO_4 solutions (Figs. 1 and 2), while the slight increases in mass are observed in pH 12, Na_2SO_4 solutions (Figs. 3 and 4). No current peaks with rapid changes in mass are observed in the cathodic potential sweep, once the passive films are formed in the anodic potential sweep, indicating that the passive films formed in both pH 3.0 and 12 solutions are stable and can not be easily reduced.

The structure and composition of passive film on nickel were studied by many researchers [10-16]. There are two controversial views of the passive film on nickel. One is that the passive film is entirely NiO with a small amount of Ni^{3+} and cation vacancies [12]. Another view is that the passive film consists of an inner layer of NiO and an outer layer of $Ni(OH)_2$ [13]. The two views may come from the difference in explanation of O1s spectra in XPS studies of passive film on nickel. Carley *et al*. [14] suggested that the O1s spectra identified with $Ni(OH)_2$ are similar to those of Ni^{3+} defects. Moreover, the STM study of passive film on single-crystal Ni (111) by Maurice et al.[15] and Zuili et al. [16] has shown that the inner part of the passive film is a crystalline NiO (111) in epitaxy with the substrate Ni (111) and the outer part of the film is an amorphous $Ni(OH)_2$.

In this study, however, for simplicity for the EQCM analysis, it is assumed that the composition of passive film on nickel is NiO. Figure 5 represents schematically the flows of Ni^{2+} and O^{2-} ions through the NiO film. At the interface between substrate nickel and NiO film, Ni is oxidized to Ni^{2+}, which is incorporated into oxide film.

$$Ni_s \rightarrow Ni_{ox}^{2+} + 2e^- \qquad (1)$$

where the subscripts, s and ox, mean the substrate and oxide film, respectively. Ni^{2+} in the film migrates outward to the interface between NiO film and solution. At the interface

between NiO film and solution, Ni^{2+} in the oxide film dissolves into solution.

$$Ni_{ox}^{2+} \rightarrow Ni_{aq}^{2+} \qquad (2)$$

where the subscript, aq, means the solution. On the other hand, the uptake of O^{2-} into oxide film at the interface between oxide film and solution proceeds with dissociation reaction of water in solution.

$$H_2O_{aq} \rightarrow O_{ox}^{2-} + 2H_{aq}^{+} \qquad (3)$$

O_{ox}^{2-} migrates inward to the interface between oxide film and substrate nickel. The dissolution of Ni^{2+} from oxide film into solution contributes to a decrease in mass, while the uptake of O^{2-} from solution into oxide film contributes to an increase in mass. The net mass loss rate, $\frac{dm_T}{dt}$, therefore, is equal to the mass loss rate due to Ni^{2+} dissolution, $\frac{dm_{Ni^{2+}}}{dt}$, minus the mass gain rate due to O^{2-} uptake, $\frac{dm_{O^{2-}}}{dt}$.

$$\frac{dm_T}{dt} = \frac{dm_{Ni^{2+}}}{dt} - \frac{dm_{O^{2-}}}{dt} \qquad (4)$$

If the partial current densities of Ni^{2+} dissolution and of O^{2-} uptake are expressed by $i_{Ni^{2+}}$ and $i_{O^{2-}}$, respectively, the following relations hold between $i_{Ni^{2+}}$ and $\frac{dm_{Ni^{2+}}}{dt}$, and between $i_{O^{2-}}$ and $\frac{dm_{O^{2-}}}{dt}$.

$$i_{Ni^{2+}} = \left(\frac{2F}{M_{Ni}}\right)\frac{dm_{Ni^{2+}}}{dt} \qquad (5a)$$

$$i_{O^{2-}} = \left(\frac{2F}{M_O}\right)\frac{dm_{O^{2-}}}{dt} \qquad (5b)$$

where M_{Ni} and M_O are the atomic weight of nickel and oxygen, respectively, and F is the Faraday constant. Furthermore, if the real current density flowed in the passive region is expressed by i_{real}, the following relation holds among i_{real}, $i_{Ni^{2+}}$ and $i_{O^{2-}}$.

$$i_{real} = i_{Ni^{2+}} + i_{O^{2-}} = \left(\frac{2F}{M_{Ni}}\right)\left[\frac{dm_{Ni^{2+}}}{dt} + \left(\frac{M_{Ni}}{M_O}\right)\frac{dm_{O^{2-}}}{dt}\right] \qquad (6)$$

We define the apparent current density, i_{app}, by Eq. (7) in order to relate to $\frac{dm_T}{dt}$.

$$i_{app} = \left(\frac{2F}{M_{Ni}}\right)\frac{dm_T}{dt} = \left(\frac{2F}{M_{Ni}}\right)\left(\frac{dm_{Ni^{2+}}}{dt} - \frac{dm_{O^{2-}}}{dt}\right) \qquad (7)$$

Since i_{real} and $\frac{dm_T}{dt}$ are known, two partial current densities of $i_{Ni^{2+}}$ and $i_{O^{2-}}$ can be obtained separately by using Eqs. (6) and (7).

Figure 6 shows the real current density, i_{real}, and the partial current densities thus obtained, $i_{Ni^{2+}}$ and $i_{O^{2-}}$, as a function of potential for the nickel electrode in pH 3.0, 0.5 M (a) and 0.1 M (b) sulfate solutions. The values of $i_{Ni^{2+}}$ and $i_{O^{2-}}$ in the active potential region between –0.1 V and 0.5 V are not meaningful because nickel hydrous oxide may precipitate as the result of active dissolution of nickel. The compact oxide film, i.e., passive film is formed at potential higher than 0.5 V where the real current density drops rapidly. Once the passive film is completely covered with the substrate nickel, Ni^{2+} dissolves through the passive film in accordance with the model proposed by Fig. 5. The values of $i_{Ni^{2+}}$ and $i_{O^{2-}}$ at potential higher than 0.5 V, therefore, may be meaningful for discussion on passivation process.

As described before, it is assumed that the composition of passive film is NiO. In the case where the passive film contains partly trivalent nickel or in the case where the passive film is partly hydrated, the values of $i_{Ni^{2+}}$ and $i_{O^{2-}}$ obtained by using Eqs. (6) and (7) provides some errors depending on the degree of Ni^{3+} content or hydration. The SO_4^{2-} concentration dependence of passivation process in pH 3.0, sulfate solution, however, may be discussed from the relative comparison between values of $i_{Ni^{2+}}$ and $i_{O^{2-}}$ in Fig. 6. At the potential higher than 0.5 V, the relatively large value of $i_{Ni^{2+}}$ in 0.5 M as compared to 0.1 M sulfate solution suggests that sulfate species in solution promote the reaction by Eq. (2). On the other hand, the situation is reversed for the value of $i_{O^{2-}}$. The zero value of

$i_{O^{2-}}$ means that the reaction by Eq. (6) attains the equilibrium and no film growth takes place, i.e., the thickness of passive film is kept constant. The relatively small value of $i_{O^{2-}}$ in 0.5 M as compared to 0.1 M sulfate solution suggests that the sulfate species in solution promote the attainment of equilibrium of the reaction by Eq. (3). Moreover, the ionic strength of solution may influence the values of $i_{Ni^{2+}}$ and $i_{O^{2-}}$ because the ionic strength of 0.5 M sulfate solution is five times as much as that in 0.1 M sulfate solution and the ionic strength controls the activity coefficient of sulfate species in solution. The mean activity coefficients, $\gamma_{\pm}$, of 0.1 M and 0.5 M sodium sulfate solutions are 0.453 and 0.270 at 298 K, respectively [17]. Consequently, the mean activities, $a_{\pm}$, are 0.045 for 0.1 M solution and 0.135 for 0.5 M solution. The promotion effects of sulfate species described above are still valid even if the ionic strength differs by a factor of five.

According to the *in-situ* infrared reflection spectroscopic study [18], the adsorption of (bi) sulfate on single-crystal nickel electrodes in pH 3.0, 0.05 M Na_2SO_4 solution were observed only in a very negative potential range prior to passive film formation. Therefore, the adsorption of (bi) sulfate on nickel thin film electrode in pH 3.0 sulfate solutions may not be so significant in the passive potential region as to influence the partial current density derived from gravimetry.

Figure 7 shows the real current density, i_{real}, and the partial current densities thus obtained, $i_{Ni^{2+}}$ and $i_{O^{2-}}$, as a function of potential for the nickel electrode in pH 12, 0.5 M (a) and 0.1 M (b) sulfate solutions. At the potential higher than 0 V, the values of $i_{Ni^{2+}}$ in pH 12, sulfate solutions are significantly lower than those in pH 3.0, sulfate solutions, independent of sulfate concentration, indicating that the reaction by Eq. (2) is retarded in alkaline solution. In alkaline solution, Ni^{2+} in the passive film dissolves into solution as ionic species of $HNiO_2^-$. The solubility limit of $HNiO_2^-$ at pH 12 is 6 x 10^{-7} M [19], while the solubility limit of Ni^{2+} at pH 3 is 6.3 x 10^6 M [19]. The low value of $i_{Ni^{2+}}$ may result from the very low

solubility limit of $HNiO_2^-$ at pH 12, sulfate solution. Moreover, the values of $i_{O^{2-}}$ in pH 12, sulfate solutions tend to increase with increasing potential in spite of rather small values of $i_{O^{2-}}$ in pH 12 as compared to pH 3.0, suggesting that it takes time for the reaction by Eq. (3) to attain the equilibrium. Although this reason is not clear, the following reaction in which hydroxide ion takes part may proceed in place of the reaction by Eq. (3).

$$OH_{aq}^- \rightarrow O_{ox}^{2-} + H_{aq}^+ \qquad (8)$$

The sulfate concentration dependences of $i_{Ni^{2+}}$ and $i_{O^{2-}}$ in pH 12, sulfate solution were not significant as compared to those in pH 3.0, sulfate solution. It is known that the specific adsorption of hydroxide ions on gold [20] or platinum [21] in alkaline solutions is stronger than that of sulfate ions. The predominant adsorption of hydroxide ions on nickel in pH 12, sulfate solution may give rise to no significant effect of sulfate concentration on $i_{Ni^{2+}}$ and $i_{O^{2-}}$.

The very low values of $i_{Ni^{2+}}$ as compared to $i_{O^{2-}}$ in pH 12, sulfate solutions are also supported by the EQCM study [22] of nickel electrode in 0.1 M KOH or NaOH solution, although the composition of passive film was assumed to be $Ni(OH)_2$. The thickness of passive film and its potential dependence may be evaluated from the $i_{O^{2-}}$ vs. E curves in the passive potential region. The difference in $i_{O^{2-}}$ between acidic and alkaline sulfate solutions would reflect directly on the difference in thickness of passive film. It seems from Figs. 6 and 7 that the thickness of passive film increases in the order of pH 3.0, 0.1 M > pH 12, 0.1 M > pH 12, 0.5 M sulfate solutions except for pH 3.0, 0.5 M sulfate solution in which the large value of $i_{Ni^{2+}}$ lowers significantly the accuracy of $i_{O^{2-}}$. At present, however, there are no pertinent literature data to confirm the above order of the film thickness.

The metal / oxide film / solution system has usually a capacitance component. Therefore, i_{real} during a potentiodynamic polarization to the anodic direction involves the

current density, i_C, for charging the capacitance. If the capacitance, C, is kept constant, i_C can be given by Eq.(8).

$$i_C = C\frac{dV}{dt} \qquad (9)$$

where $\frac{dV}{dt}$ is the potential sweep rate. The exact capacitance values for the metal / oxide film / solution systems are unknown but may be less than those of electric double layer (C_D = 0.4 F m^{-2}) for the oxide free- metal / solution systems. However, even if assuming that the capacitance for the nickel / passive film / solution system is equal to C_D = 0.4 F m^{-2}, i_C is 0.8 μA cm^{-2}. The contributions of i_C to i_{real} , therefore, are only less than 1% in pH 3, sulfate solution and 2-4 % in pH 12, sulfate solution. The separation of $i_{Ni^{2+}}$ and $i_{O^{2-}}$ from i_{real} may be valid since the contribution of i_C is negligibly small within experimental errors of i_{real}.

4. Conclusions

Passivation process of the electroplated nickel thin film in 0.5 M and 0.1 M sulfate solutions of pH 3.0 and 12 was analyzed by using an EQCM. The following conclusions were drawn.

a) The separation of real current density, i_{real}, into two partial current densities of Ni^{2+} from passive film into solution, $i_{Ni^{2+}}$, and of oxygen uptake from solution into passive film, $i_{O^{2-}}$, could be achieved from comparison between the voltammogram and gravimetrical curve.

b) The separated $i_{Ni^{2+}}$ and $i_{O^{2-}}$ in the passive region depended sensitively on solution pH. In pH 3.0, sulfate solution, the sulfate species promoted $i_{Ni^{2+}}$ and retarded $i_{O^{2-}}$. The lower value of $i_{Ni^{2+}}$ in pH 12 than pH 3.0, sulfate solution may be ascribed to the very low solubility of $HNiO_2^-$ that is a stable species in alkaline solution.

c) The sulfate concentration dependences of $i_{Ni^{2+}}$ and $i_{O^{2-}}$ in pH 12, sulfate solution were not significant as compared to those in pH 3.0, sulfate solution, which may come from the

predominant adsorption of hydroxide ions on nickel in alkaline solution.

References

[1] M. Seo, K. Yoshida and K. Noda, *Mater. Sci. & Eng.*, **A198** (1995) 197-203.

[2] M. Seo, K. Yoshida and K. Noda, *Mater. Sci. Forum*, **192-194** (1995) 755-764.

[3] K. J. Vetter and F. Gorn, *Electrochim. Acta*, **18** (1973) 321-326.

[4] L. Grasjö, M. Seo and N. Sato, *Corros. Sci.*, **31** (1990) 299-304.

[5] M. Seo and H. Tsuda, *Electrochemical Society Proc.*, **99-27** (1999) 280-289.

[6] A. Grzegorzewski and K. E. Heusler, *J. Electroanal. Chem.*, **228** (1987) 455-470.

[7] P. Schmutz and D. Landolt, *Electrochim. Acta*, **45** (1999) 899-911.

[8] C.-O. A. Olsson and D. Landolt, *J. Electrochem. Soc.,* **148** (2001) B348-B449.

[9] D. Hamm, C.-O. A. Olsson and D. Landolt, *Corros. Sci.*, **44** (2002) 1009-1025.

[10] N. Sato and K. Kudo, *Electrochim. Acta*, **19** (1974) 461-470.

[11] T. Ohtsuka and K. E. Heusler, *J. Electroanal. Chem.* , **102**(1979) 175-187.

[12] B. MacDougall, *Corros. Sci.,* **28** (1988) 211-216.

[13] P. Marcus, J. Oudar and I. Olefjord, *J. Microsc. Spectrosc. Electron,* **4** (1979) 63-72.

[14] A. F. Carely, R. P. Chalker and M. W. Roberts, *Proc. R. Soc. Lond. Ser.* **A399**(1985) 167-179.

[15] V. Maurice, H. Talah and P. Marcus, *Surface Science*, **304**(1994) 98-108.

[16] D. Zuili, V. Maurice and P. Marcus, *J. Electrochem. Soc.*,**147** (2000) 1393-1400.

[17] D. Dobos, "*Electrochemical Data*",, Elsevier Scientific Publishing Company (1975) p. 196.

[18] M. Nakamura, N. Ikemiya, A. Iwasaki, Y. Suzuki and M. Ito, *J. Electroanal. Chem.*, **566** (2004) 385-391.

[19] M. Pourbaix, " *Atlas of Electrochemical Equilibria in Aqueous Solutions*", NACE

(1974) p. 330.

[20] M. Seo, X. C. Jiang and N. Sato, *J. Electrochem. Soc*., **134**(1987) 3094 -3098.

[21] M. Seo and Y. Serizawa, *J. Electrochem. Soc.,* **150**(2003) E472-E476.

[22] M. Grde´n, K. Klimek and A. Czerwi´nski, *J. Solid State Electrochem.*, **8** (2004) 390-397.

Figure Captions

Fig.1 Voltammogram and gravimetrical curve of nickel thin film electrode in 0.5 M sulfate solution of pH 3.0.

Fig. 2 Voltammogram and gravimetrical curve of nickel thin film electrode in 0.1 M sulfate solution of pH 3.0.

Fig. 3 Voltammogram and gravimetrical curve of nickel thin film electrode in 0.5 M sulfate solution of pH 12.

Fig. 4 Voltammogram and gravimetrical curve of nickel thin film electrode in 0.1 M sulfate solution of pH 12.

Fig. 5 Model for passivation process of nickel.

Fig. 6 Voltammograms, partial current densities of nickel dissolution, $i_{Ni^{2+}}$, and partial current densities of film growth, $i_{O^{2-}}$, for nickel thin film electrode in (a) 0.5 M and (b) 0.1 M sulfate solutions of pH 3.0.

Fig. 7 Voltammograms, partial current densities of nickel dissolution, $i_{Ni^{2+}}$, and partial current densities of film growth, $i_{O^{2-}}$, for nickel thin film electrode in (a) 0.5 M and (b) 0.1 M sulfate solutions of pH 12.

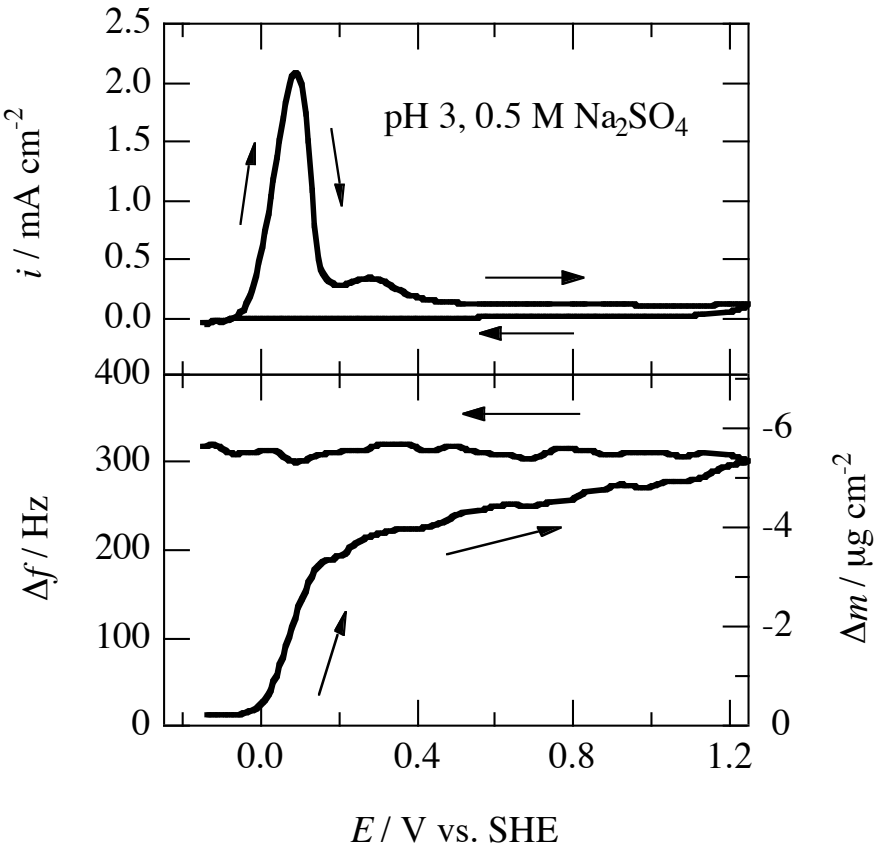

Fig.1 Voltammogram and gravimetrical curve of nickel thin film electrode in 0.5 M sulfate solution of pH 3.0.

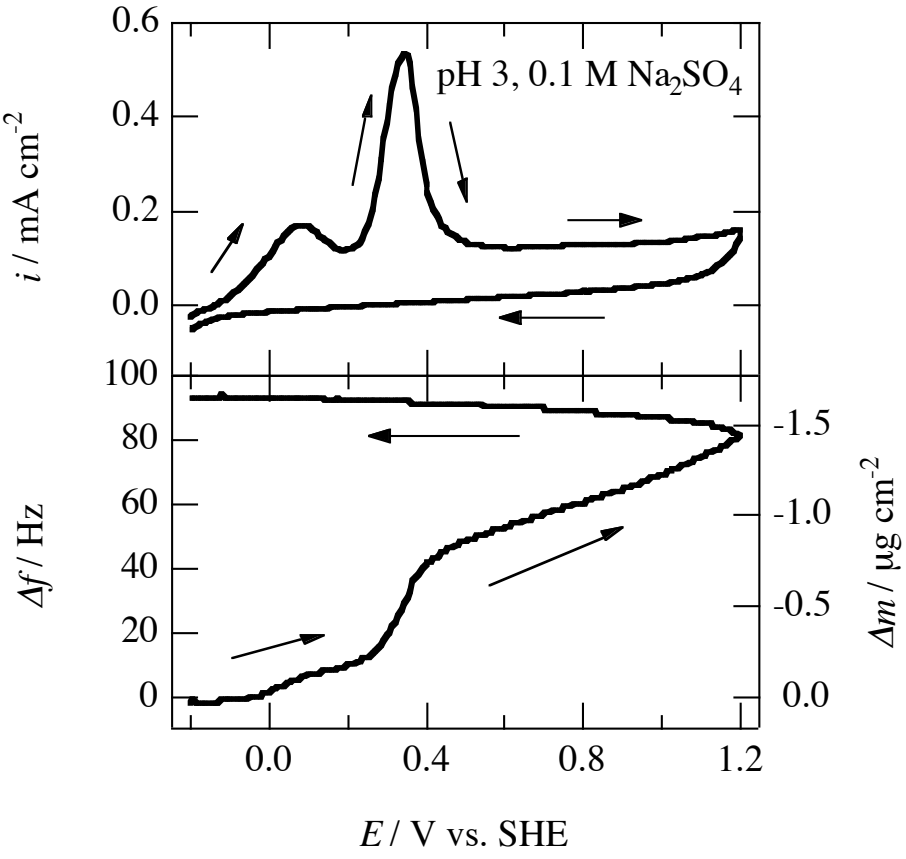

Fig. 2 Voltammogram and gravimetrical curve of nickel thin film electrode in 0.1 M sulfate solution of pH 3.0.

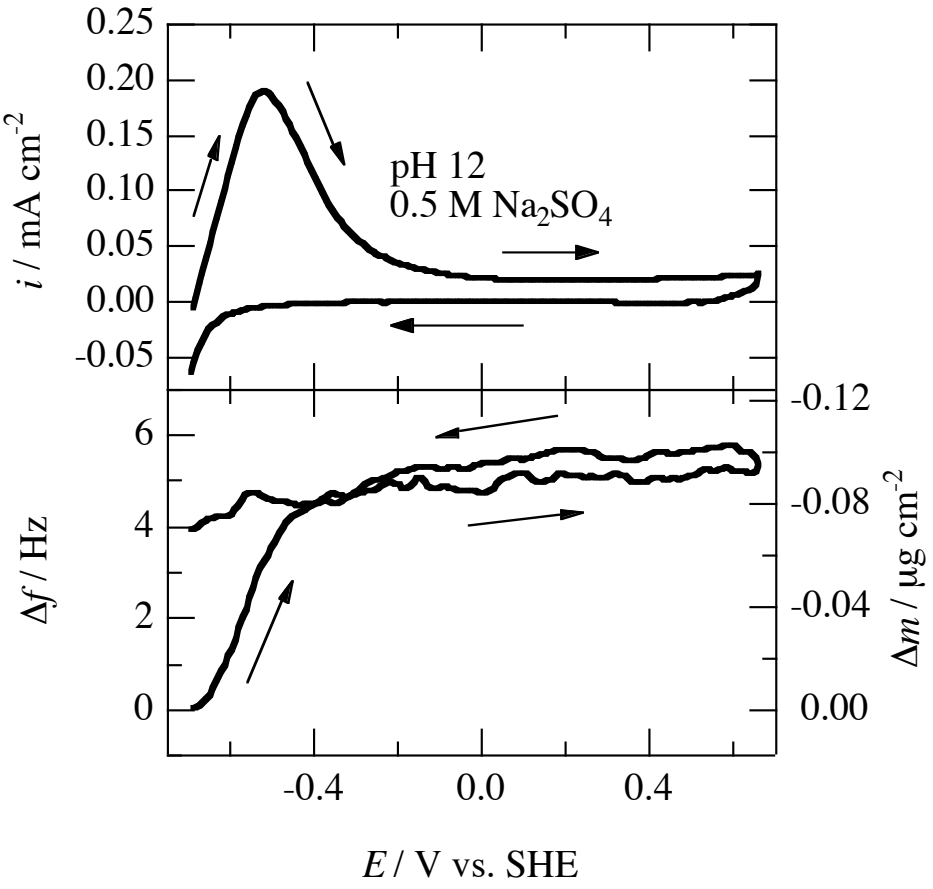

Fig. 3 Voltammogram and gravimetrical curve of nickel thin film electrode in 0.5 M sulfate solution of pH 12.

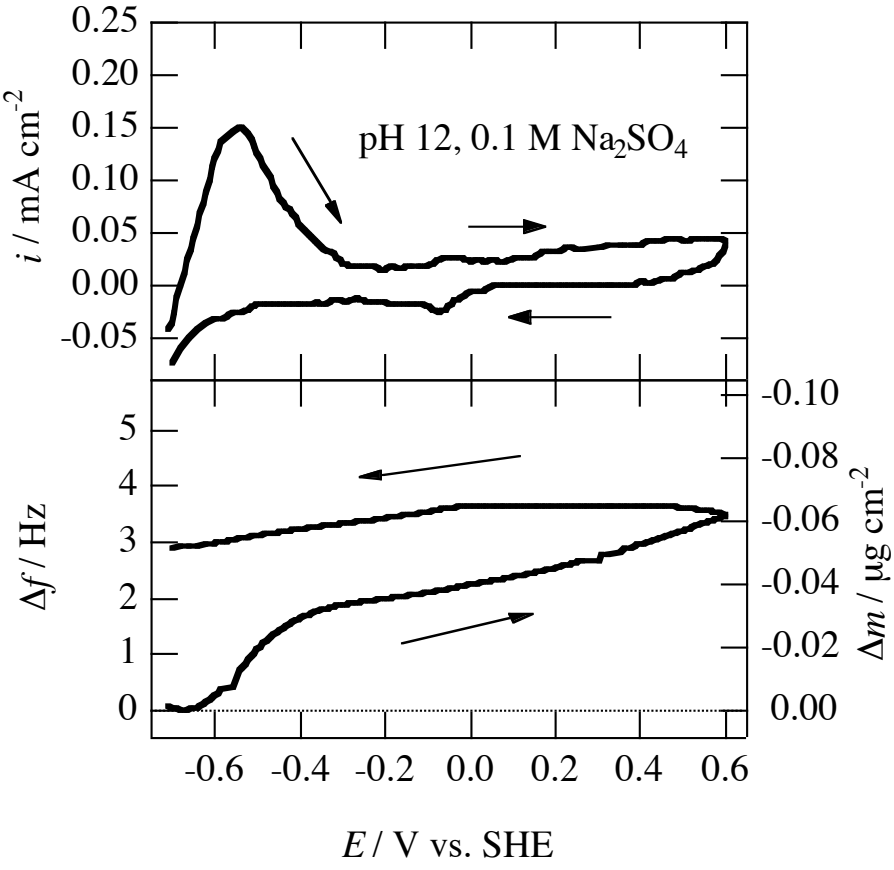

Fig. 4 Voltammogram and gravimetrical curve of nickel thin film electrode in 0.1 M sulfate solution of pH 12.

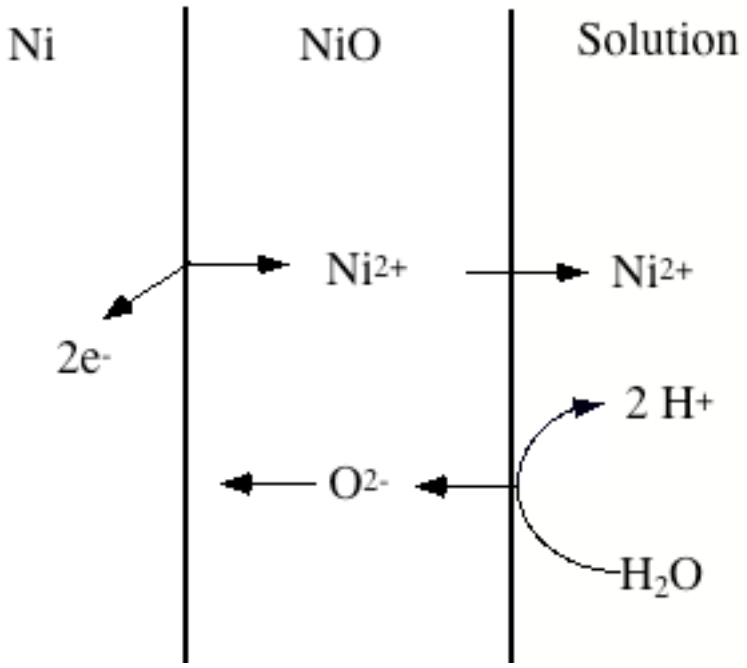

Fig. 5 Model for passivation process of nickel.

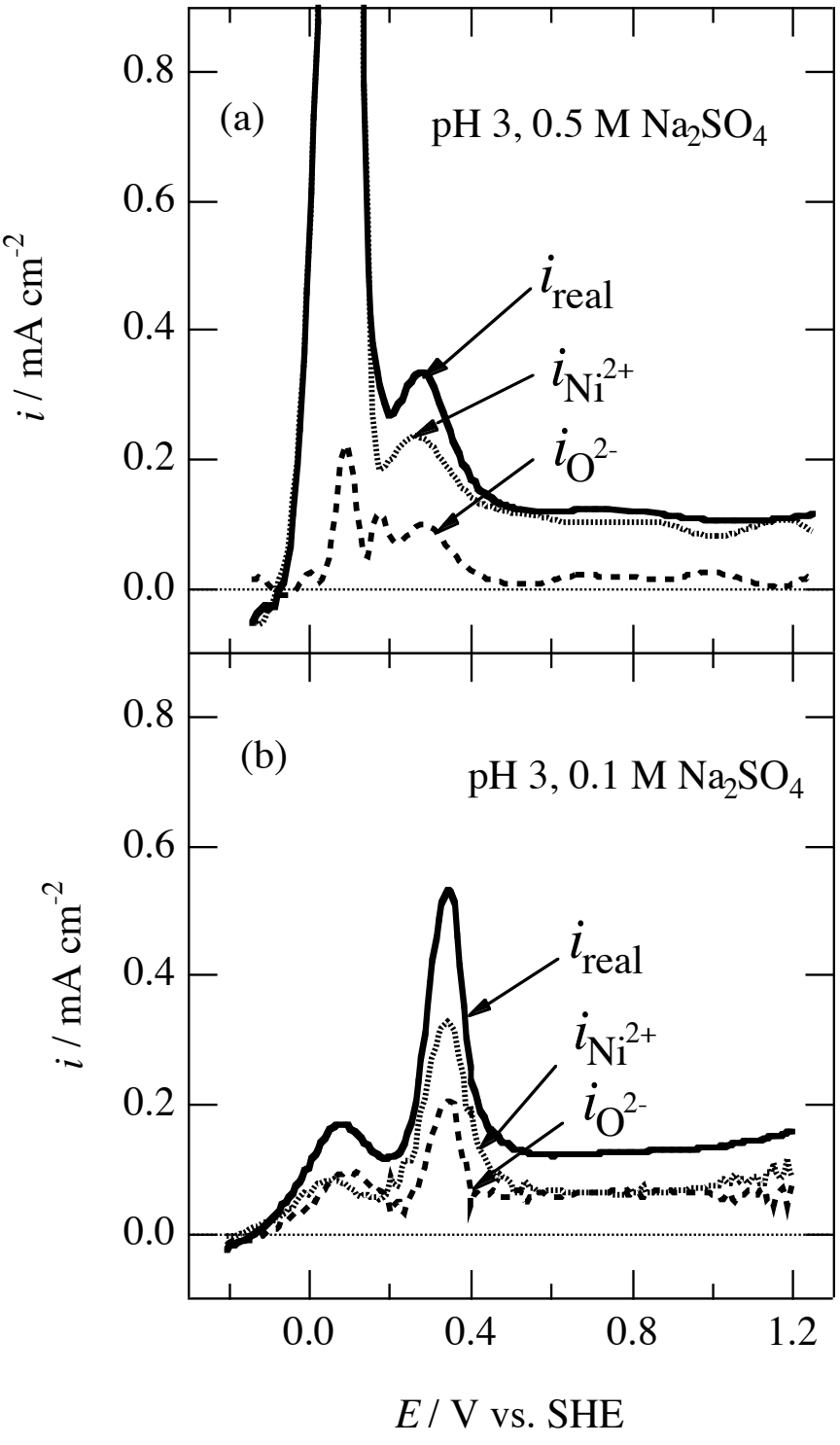

Fig. 6 Voltammograms, partial current densities of nickel dissolution, $i_{Ni^{2+}}$, and partial current densities of film growth, $i_{O^{2-}}$, for nickel thin film electrode in (a) 0.5 M and (b) 0.1 M sulfate solutions of pH 3.0.

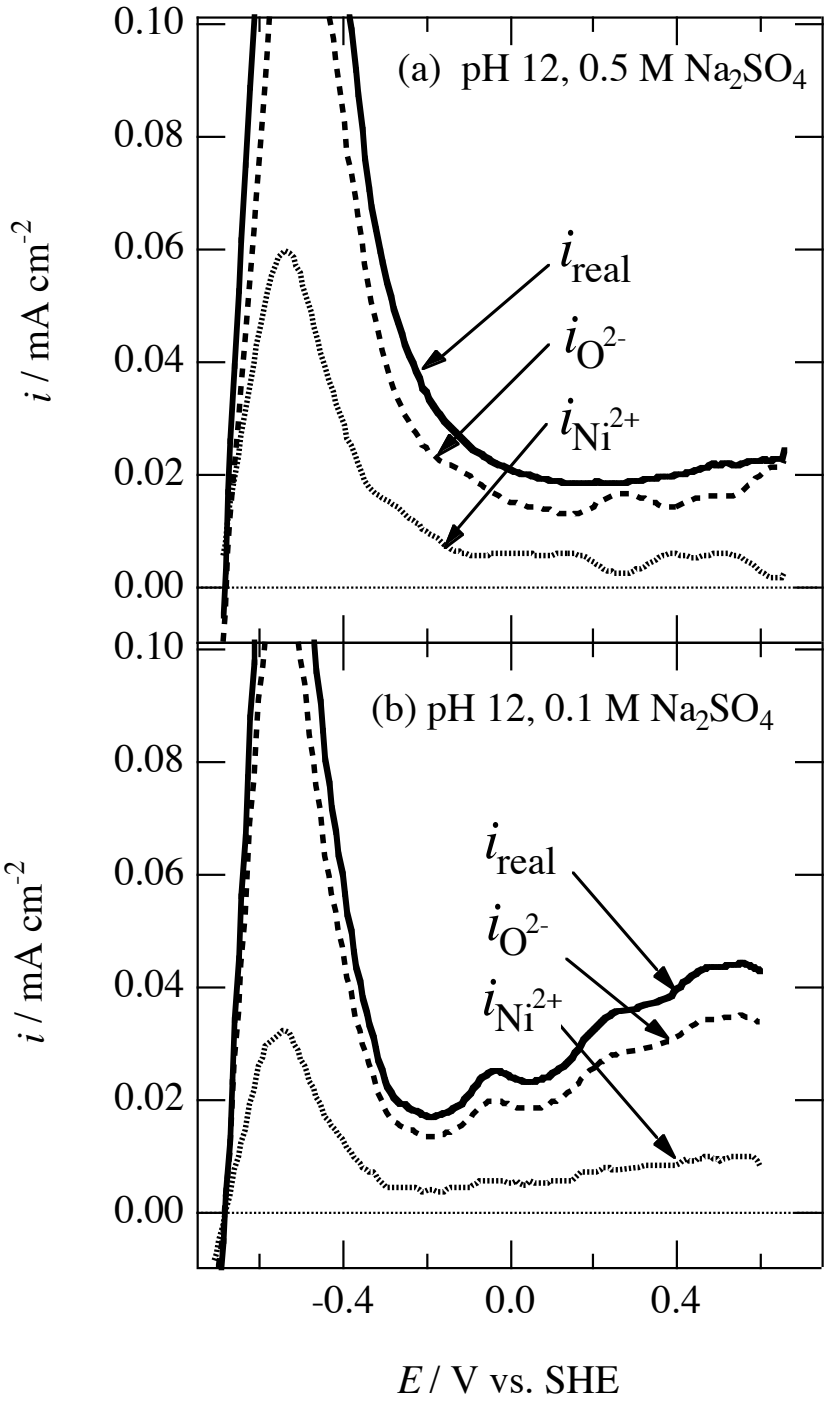

Fig. 7 Voltammograms, partial current densities of nickel dissolution, $i_{Ni^{2+}}$, and partial current densities of film growth, $i_{O^{2-}}$, for nickel thin film electrode in (a) 0.5 M and (b) 0.1 M sulfate solutions of pH 12.